SUPPORTING INFORMATION

Enhanced Thermal Transport Properties of Heat Spreader Assembled by Non-covalent Functionalized Graphene

Li Ren [†,#], Mengjie Wang [‡,#], Zhouqiao Wei [†,#], Jingzhen Cheng [†], Kuo Liu [†], Lulu Pan [†], Li Lao [†], Shaorong Lu [*,†], and Jinhong Yu [*,†,‡]

[†] Key Laboratory of New Processing Technology for Nonferrous Metals and Materials, Ministry of Education, School of Material Science and Engineering, Guilin University of Technology, Guilin, 541004, China.

[‡] Key Laboratory of Marine Materials and Relater Technologies, Zhejiang Key Laboratory of Marine Materials and Protective Technologies, Ningbo Institute of Materials Technology and Engineering, Chinese Academy of Sciences, Ningbo 315201, China.

[⊥] Center of Materials Science and Optoelectronics Engineering, University of Chinese Academy of Sciences, Beijing 100049, China.

*Corresponding authors E-mails: **lushaor@163.com (S. R. Lu)**; **yujinhong@nimte.ac.cn (J. H. Yu)**.

[#]These authors contributed equally.

SUPPLEMENT

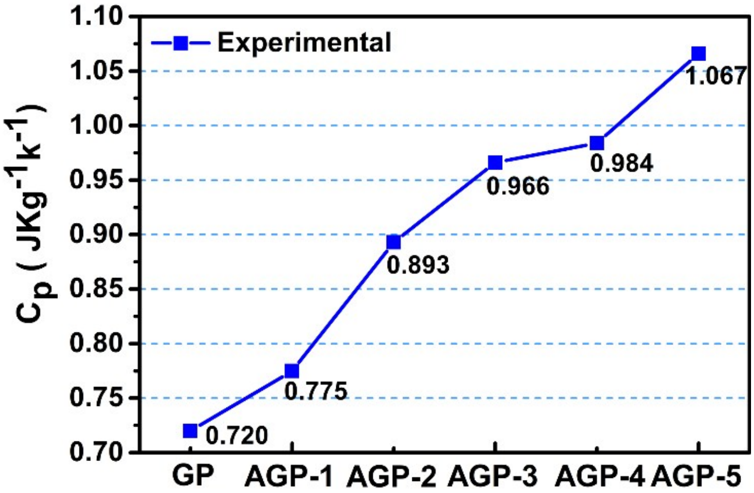

Figure S1 The Specific heat capacity (*Cp*) of GP and AGPs with various APBI loadings at room temperature.

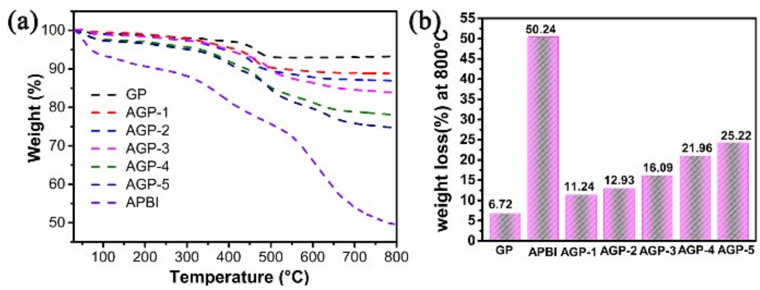

Figure S2 (a) TGA curves and (b) weight loss of GP, APBI, AGP-1, AGP-2, AGP-3, AGP-4 and AGP-5 at 800 °C.

It can be seen from the Figure S2 that GP, APBI, AGP-1, AGP-2, AGP-3, AGP-4 and AGP-5 had a 6.72 %, 50.24 %, 11.24 %, 12.93 %, 16.09 %, 21.86 % and 25.22 % weight loss at 800 °C, respectively. Thus, it was figured out according to the following equation that AGP-1 contained about 89.64wt% GNS and 10.36wt% APBI.

$$6.72x + 50.24y = 11.24 \quad (1)$$

$$x + y = 1 \quad (2)$$

x and y are weight loss percentage of GNs and APBI, respectively. Similarly, the AGP-2, AGP-3, AGP-4 and AGP-5 contain 14.22 wt%, 21.45 wt%, 34.65 wt% and 42.36 wt% APBI, respectively.

Figure S3 The aqueous dispersion (2.5×10^{-4} g/mL) of APBI, GNs, AG-1, AG-2, AG-3, AG-4 and AG-5 after standing for 12 h.

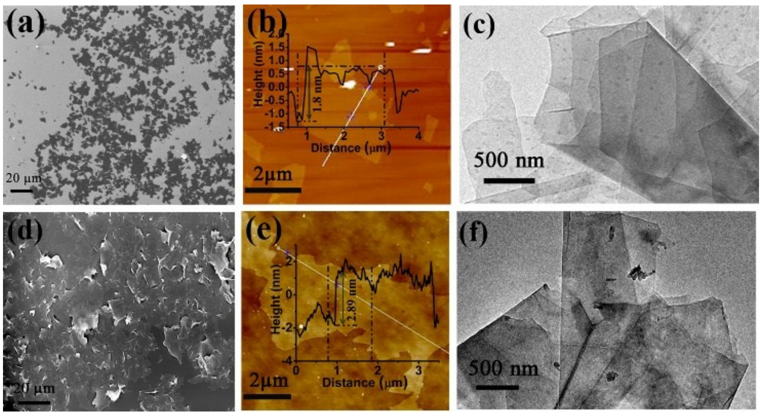

Figure S4 SEM, AFM and TEM images of GNs (a, b, c) and AG (d, e, f).

Figure S4 shows the SEM, AFM and TEM images of GNs and APBI functionalized graphene nanosheets (AG). The average size of the GNs was approximately 7μm as shown in Figure S4(a). Figure S4(d) displays that most of the nanosheets are seriously wrinkled and aggregated together, indicating that APBI acts as an adhesive to connect GNs. And the thickness of GNs was measured to be 1.8 nm (Figure S4(b)), which indicated that the graphene has five or six layers stacked together. After APBI was attached into the GNs via π-π stacking interaction, the thickness of AG was increased to 2.89 nm (Figure S4(e)), indicating the strong π-π stacking interactions exist between APBI and GNs.[1] In addition, the morphology of GNs and AG were demonstrated by the TEM. As shown in Figure S4(c), it can be seen that the GNs was several layers consistent with the AFM characterization and the edge of the GNs were rolled up. And the surface of AG is darker than GNs and some APBI were attached on to the GNs as shown in Figure S4 (f), suggesting that the successful π-π stacking interaction between APBI and GNs.

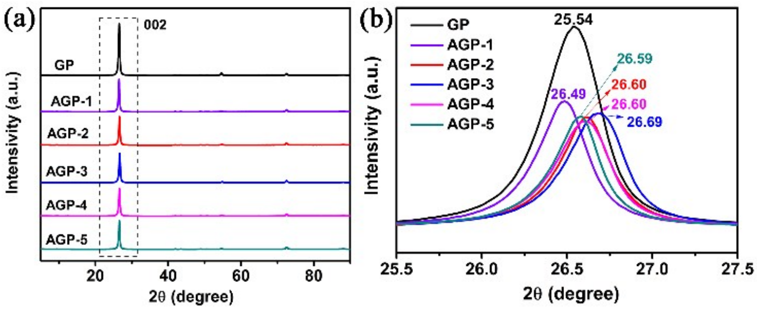

Figure S5 (a) XRD curves of GP, AGP-1, AGP-2, AGP-3, AGP-4 and AGP-5. (b) The 002 peak of GP, AGP-1, AGP-2, AGP-3, AGP-4 and AGP-5 in range of 25.5~27.5 degree.

Figure S6 Digital photographs of GP, AGP-1, AGP-2, AGP-3, AGP-4 and AGP-5 (unpressured).

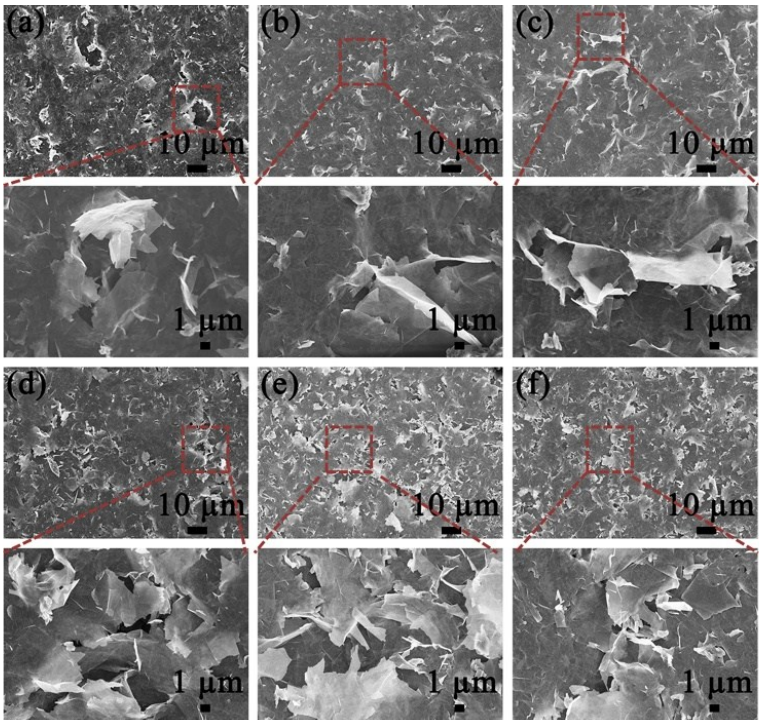

Figure S7 SEM images of the surface of (a) GP, (b) AGP-1, (c) AGP-2, (d) AGP-3, (e) AGP-4 and (f) AGP-5.

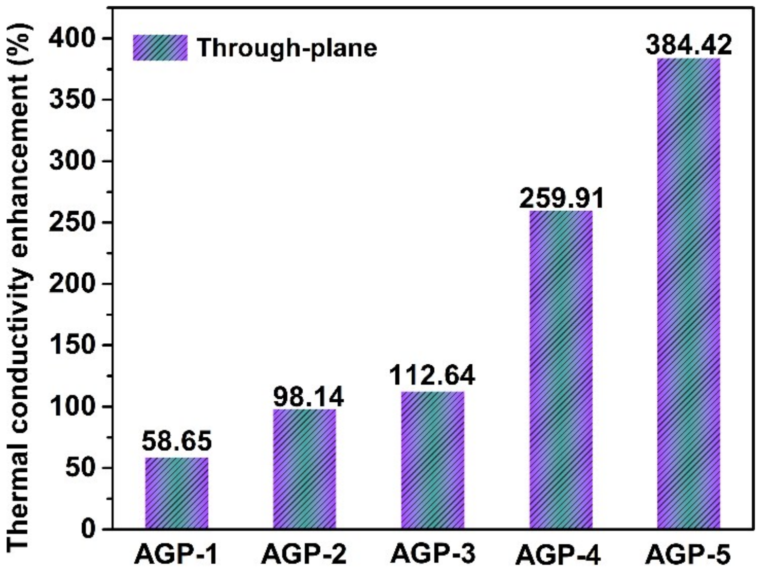

Figure S8 Thermal conductivity enhancement of AGPs for the through-plane directions.

Table S1. The thermal conductivities and mechanical properties of Graphene-based papers.

Reference and year	**materials**	**$Tc_{\parallel}^{a}$ ($W\ m^{-1}\ K^{-1}$)**	**$Tc_{\perp}^{b}$ ($W\ m^{-1}\ K^{-1}$)**	**Tensile strength (MPa)**	**Toughness ($MJ\ m^{-3}$)**
2008[2]	RGO-PB	—	—	8.4	—
2011[3]	xGnP	178	1.28	—	—
2013[4]	AgNWs/graphene paper	—	—	—	—
2013[5]	rGO-PCDO	—	—	129.6	3.91
2013[6]	rGO-SL	—	—	300.0	2.80
2014[7]	rGO-PAPB	—	—	382.0	7.50
2014[8]	rGO-PDA	—	—	204.9	4.00
2014[9]	G-GF	977	—	15.3	—
2014[10]	TPA-rGO	—	—	~125	~1.0
2015[11]	rGO-FPEG	—	—	45.0	—
2015[12]	rGO-CS	—	—	526.7	17.69
2015[13]	rGO-DWNT-PCDO	—	—	374.1	9.20
2015[14]	rGO-MoS_2-TPU	—	—	235.0	6.90
2015[15]	rGO-MMT-PVA	—	—	356.0	7.50
2015[16]	PVA-SRGO	—	—	252	—
2015[17]	Ca-GP	331.8	—	—	—
2015[18]	CNR/graphene paper	890	5.81	—	—
2016[19]	rGO-NFC-PCDO	—	—	314.6	9.8
2016[20]	rGO-DWNTs-PVA	—	—	384.2	19.3
2017[21]	CNT/G	1388.7	0.16	—	—
2017[22]	rGO-CNT	804.24	0.06	—	—
2017[23]	rGO-AP-DSS	—	—	538.8	16.1
2017[24]	rGO/Al-CMC-GO	—	—	586.6	12.1
2017[25]	rGO-PVA	—	—	150.9	8.5
2017[26]	rGO-CNC	—	—	765	15.64
2018[27]	SBG	—		821	20
2018[28]	SBG			945	20.6
2018[29]	GFs	3200	—	78	—
2018[30]	rGO-CNR film	1820.4	4.60	31.6	—
2019[31]	rGO-WSCA	—	—	499.3	9.6
This work	**AGP-2**	**289.37**	**2.73**	**47.9**	**0.34**
	AGP-5	**231.68**	**6.67**	**19.8**	**0.16**

Referance

1. Alijani, V.; Li, C.; Feng, X. L.; Müllen, K. Composites of Graphene with Large Aromatic Molecules. *Adv.Mater.* **2009**, *21*, 3191-3195.

2. Xu, Y. X.; Bai, H.; Lu, G. W.; Li, C.; Shi, G. Q. Flexible Graphene Films via the Filtration of Water-Soluble Noncovalent Functionalized Graphene Sheets. *J. Am. Chem. Soc*. **2008**, *130*, 5856-5857.

3. Xiang, J. L.; Drzal, L. Thermal conductivity of exfoliated graphite nanoplatelet paper. *Carbon* **2011**, *49*, 773-778.

4. Chen, J.; Bi, H.; Sun, S. R.; Tang, Y. F.; Zhao, W.; Lin, T. Q.; Wan, D. Y.; Huang, F. Q.; Zhou, X. D.; Xie, X. M.; Jiang, M. H. Highly Conductive and Flexible Paper of 1D Silver-Nanowire-Doped Graphene. *ACS Appl. Mater. Interfaces* **2013**, *5*, 1408-1413.

5. Cheng, Q. F.; Wu, M. X.; Li, M. Z.; Jiang, L.; Tang, Z. Y. Ultratough Artificial Nacre Based on Conjugated Cross-Linked Graphene Oxide. *Angew. Chem. Int. Ed*. **2013**, *52*, 3750-3755.

6. Hu, K. S.; Tolentino, L. S.; Kulkarni, D. D.; Ye, C. H.; Kumar, S.; Tsukruk, V. V. Written-in Conductive Patterns on Robust Graphene Oxide Biopaper by Electrochemical Microstamping. *Angew. Chem. Int. Ed*. **2013**, *52*, 13784-13788.

7. Zhang, M.; Huang, L.; Chen, J.; Li, C.; Shi, G. Q. Ultratough, Ultrastrong, and Highly Conductive Graphene Films with Arbitrary Sizes. *Adv. Mater*. **2014**, *26*, 7588-7592.

8. Cui, W.; Li, M. Z.; Liu, J. Y.; Wang, B.; Zhang, C.; Jiang, L.; Cheng, Q. F. A Strong Integrated Strength and Toughness Artificial Nacre Based on Dopamine Cross-Linked Graphene Oxide. *ACS Nano* **2014**, *8*, 9511-9517.

9. Kong, Q. Q.; Liu, Z.; Gao, J. G.; Chen, C. -M.; Zhang, Q.; Zhou, Q. M.; Tao, Z. -C.; Zhang, X. -H.; Wang, M. -Z.; Li, F.; Cai, L. Hierarchical Graphene-Carbon Fiber Composite Paper as a Flexible Lateral Heat Spreader. Adv. Funct. Mater. **2014**, *24*, 4222-4228.

10. Chow, P. K.; Eksik, O.; Koratkar, K. Mechanical Property Enhancement of Layered Reduced Graphene Oxide Papers by Non-Covalent Modification with Terephthalic Acid. Part. Part. Syst. Charact. **2014**, *31*, 337-341.

11. Zhang, J. Z.; Xu, Y. H.; Cui, L.; Fu, A. P.; Yang, W. R.; Barrow, C.; Liu, J. Q. Mechanical Properties of Graphene Films Enhanced by Homo-Telechelic Functionalized Polymer Fillers via π-π Stacking Interactions. Composites Part A **2015**, *71*, 1-8.

12. Wan, S. J.; Peng, J. S.; Li, Y. C.; Hu, H.; Jiang, L.; Cheng, Q. F. Use of Synergistic Interactions to

Fabricate Strong, Tough, and Conductive Artificial Nacre Based on Graphene Oxide and Chitosan. *ACS Nano* **2015**, *9*, 9830-9836.

13. Gong, S. S.; Cui, W.; Zhang, Q.; Gao, A. Y.; Jiang, L.; Cheng, Q. F. Integrated Ternary Bioinspired Nanocomposites via Synergistic Toughening of Reduced Graphene Oxide and Double-Walled Carbon Nanotubes. *ACS Nano* **2015**, *9*, 11568-11573.

14. Wan, S. J.; Li, Y.; Peng, J.; Hu, H.; Cheng, Q. F.; Jiang, L. Synergistic Toughening of Graphene Oxide-Molybdenum Disulfide-Thermo-Plastic Polyurethane Ternary Artificial Nacre. *ACS Nano* **2015**, *9*, 708-714.

15. Ming, P.; Song, Z. F.; Gong, S. S.; Zhang, Y. Y.; Duan, J. L.; Zhang, Q.; Jiang, L.; Cheng, Q. F. Nacre-inspired integrated Nanocomposites with Fire Retardant Properties by Graphene Oxide and Montmorillonite. *J. Mater. Chem. A*. **2015**, *3*, 21194-21200.

16. Mo, S. B.; Peng, L.; Yuan, C. Q.; Zhao, C. Y.; Tang, W.; Ma, C. L.; Shen, J. X.; Yang, W. B.; Yu, Y. H.; Min, Y.; Epstein. A. J. Enhanced Properties of Poly(vinyl alcohol) Composite Films with Functionalized Graphene. *RSC Adv*. **2015**, *5*, 97738-97745.

17. Yu, W.; Xie, H. Q.; Chen, L. F.; Zhao, J. C.; Li, F. X. Modified Graphene Papers with Alkaline Earth Metal Ions Endowed with High Heat Transfer Properties. *Thin Solid Films* **2015**, *597*, 77-82.

18. Zhang, J. W.; Shi, G.; Jiang, C.; Ju, S.; Jiang, D. Z. 3D Bridged Carbon Nanoring/Graphene Hybrid Paper as a High-Performance Lateral Heat Spreader. *Small* **2015**, *11*, 6197-6204.

19. Duan, J. L.; Gong, S. S.; Gao, Y.; Xie, X. L.; Jiang, L.; Cheng, Q. F. Bioinspired Ternary Artificial Nacre Nanocomposites Based on Reduced Graphene Oxide and Nanofibrillar Cellulose. *ACS Appl. Mater. Interfaces* **2016**, *8*, 10545-10550.

20. Gong, S. S.; Wu, M. X.; Jiang, L.; Cheng, Q. F. Integrated Ternary Artificial Nacre via Synergistic Toughening of Reduced Graphene Oxide/Double-Walled Carbon Nanotubes/Poly(Vinyl Alcohol). *Mater. Res. Express* **2016**, *3*, 075002.

21. Lu, F. F.; Zhang, J.; Luo, J.; Gong, W. B.; Li, C. W.; Zhang, K.; Hu, M.; Yao, Y. G. Enhanced Thermal Conductivity of Free-Standing 3D Hierarchical Carbon Nanotube-Graphene Hybrid Paper. *Compos. Part A* **2017**, *102*, 1-8.

22. Pan, T. W.; Kuo, W. S.; Tai, N. H. Tailoring Anisotropic Thermal Properties of Reduced Graphene Oxide/Multi-Walled Carbon Nanotube Hybrid Composite Films. *Compos. Sci. Technol*. **2017**, *151*, 44-51.

23. Ni, H.; Xu, F. Y.; Tomsia, A. P.; Saiz, E.; Jiang, L.; Cheng, Q. F. Robust Bioinspired Graphene Film via π-π Cross-linking. *ACS Appl. Mater. Interfaces* **2017**, *9*, 24987-24992.

24. Shahzadi, K.; Zhang, X. M.; Mohsin, I.; Ge, X. S.; Jiang, Y. J.; Peng, H.; Liu, H. Z.; Li, H.; Mu, X. D. Reduced Graphene Oxide/Alumina, A Good Accelerant for Cellulose-Based Artificial Nacre with Excellent Mechanical, Barrier, and Conductive Properties. *ACS Nano* **2017**, *11*, 5717-5725.

25. Zhang, N. F.; Yang, M.; Zhao, Q.; Gao, W. W.; Xie, T.; Bai, H. Superstretchable Nacre-Mimetic Graphene/Poly(Vinyl Alcohol) Composite Film Based on Interfacial Architecture Engineering. *ACS Nano* **2017**, *11*, 4777-4784.

26. Wen, Y. Y.; Wu, M. M.; Zhang, M.; Li, C.; Shi, G. Q. Topological Design of Ultrastrong and Highly Conductive Graphene Films. *Adv. Mater.* **2017**, *29*, 1702831.

27. Wan, S. J.; Fang, S. L.; Jiang, L.; Cheng, Q. F.; Baughman, R. H. Strong, Conductive, Foldable Graphene Sheets by Sequential Ionic and π Bridging. *Adv. Mater*. **2018**, *30*, 1802733.

28. Wan, S. J.; Li, Y. C.; Mu, J. K.; Aliev, A. E.; Fang, S. L.; Kotov. N. N.; Jiang, L.; Cheng, Q.F.; Baughman, R. H. Sequentially Bridged Graphene Sheets with High Strength, Toughness, and Electrical Conductivity. *PANS* **2018**, *115*, 5359-5364.

29. Wang, N.; Samani, K. S.; Li, H.; Dong, L.; Zhang, Z. W.; Su, P.; Chen, S. J.; Chen, J.; Huang, S. R.; Yuan, G. J.; Xu, X. F.; Li, B.W.; Leifer, K.; Ye, L. L.; Liu, J. Tailoring the Thermal and Mechanical Properties of Graphene Film by Structural Engineering. *Small* **2018**, *14*, 1801346.

30. Meng, X.; Pan, H.; Zhu, C. L.; Chen, Z. X.; Lu, T.; Xu, D.; Li, Y.; Zhu, S. M. Coupled Chiral Structure in Graphene-Based Film for Ultrahigh Thermal Conductivity in Both In-Plane and Through-Plane Directions. *ACS Appl. Mater. Interfaces* **2018**, *10*, 22611-22622.

31. Pang, J. H.; Wang, X. P.; Li, L.; Wu, M.; Jiang, J.; Ji, Z.; Yu, S. T.; Yu, H. L.; Zhang, X. M. Tough and Conductive bio-based artificial Nacre via Synergistic Effect Between Water-Soluble Cellulose Acetate and Graphene. *Carbohyd. Polym.* **2019**, *206*, 319-327.